ECOSYSTEM IMPACTS OF WOODY ENCROACHMENT IN TEXAS: A SPATIAL ANALYSIS USING AVIRIS

Roberta E. Martin,[1,2] Gregory P. Asner[2,3]

1. Introduction

Woody encroachment, the increase of woody plant density relative to herbaceous vegetation, has been documented in drylands of Texas as well as worldwide (Archer 1994, Harrington and Harman 1995, Moleele et al. 2002). Over-grazing, fire suppression and climate change are implicated in the shift from open grasslands to ecosystems now populated by trees and shrubs (Scholes and Archer 1997, Archer et al. 2001), such as *Prosopis glandulosa* var. glandulosa (honey mesquite) in north Texas (Teague et al. 1997, Ansley et al. 2001, Asner et al. 2003a). Several studies have examined changes in ecosystem properties accompanying woody vegetation encroachment in the Southwest U.S., with research focused on increases in plant and soil carbon (C) and nitrogen (N) stores (Hoffman and Jackson 2000, Asner et al. 2003a), isotopic shifts in these pools (Boutton 1999, Archer et al. 2001), and increases in N cycling rates (Rundel et al. 1982, Hibbard et al. 2001). However, little is known regarding the impact of woody encroachment on N trace gas emissions from dryland regions such as Texas.

NOx is produced in the soil during the processes of nitrification and denitrification (Firestone and Davidson 1989). The total N efflux from soils is most directly influenced by the internal cycling of N, which at a regional-scale, is controlled by the inputs and availability of N from vegetation via litterfall and subsequent decomposition (Robertson et al. 1989). Although plot-scale studies are critical to understanding controls over N oxide emissions, regionalization of the measurements is impeded by spatial variation in the factors contributing most to N cycling processes: soil properties (affecting soil moisture regimes and N stocks) and vegetation cover (affecting litter inputs and N uptake). While broad patterns in ecosystem structure and vegetation composition co-vary with general patterns of trace gas emissions (Matson 1997), there is no easily measured index of N availability that can be applied for regional-scale studies of N oxide fluxes.

Remote sensing is arguably the only approach available to develop a spatially-explicit understanding of ecosystem processes. More specifically, remotely detectable spatial patterns in the distal controls over soil N properties, such as vegetation cover, land use and soil type (Robertson et al. 1989), should be exploited for regional studies of N oxide emissions. The woody encroachment phenomenon provides an opportunity to test the strength of the relationship between N oxide emissions and those factors controlling the fluxes that can be remotely measured. If such linkages can be firmly established, and if the spatial pattern of distal controls is relevant, then the combination of field measurements and remote sensing offers to improve regional-scale N oxide estimates.

The paper presents the utility of linking field based sampling of soil NOx emissions with very high resolution remote sensing estimates of woody vegetation cover from the NASA AVIRIS, Airborne Visible-Infrared Imaging Spectrometer (Green et al. 1998, Asner and Green 2001) and automated spectral mixture analysis (Asner and Lobell 2000, Asner and Heidebrecht 2002) that provide a means to spatially extrapolate soil NOx emissions to the regional scale.

2. Study site.

The study site was located on the Waggoner Ranch in North Texas (33°50'N, 99°02'W; Figure 1). The region is temperate mixed –grass savanna with a mean annual temperature of 17 °C. Mean annual precipitation (640 mm) is bimodally distributed, with peaks in May and September. Topography of the region is gentle to moderately sloping (< 4%); elevation ranges from 355-370 m. Soils on lowland areas are fine, mixed thermic, Typic Paleustolls of the Tillman association, developed from Permian clay and shale parent material (SCS 1962). Upland soils are dominated by shallower Vernon series clay loams and intermittently exposed red-bed clays and shales. Vegetation is dominated by a mixture of native grasses (both C_3 and C_4) and a P. glandulosa (mesquite) overstory comprising > 95% of all woody cover and density (Hughes et al. 1999). While historical vegetation of the region was grassland and open savanna in the 1950s, in association with an increase in cattle grazing, the density of *P. glandulosa* increased to the point where brush management efforts were employed throughout the region (Fisher et al. 1959, Teague et al. 1997, Ansley et al. 2001). These efforts have continued to the present (Teague et al. 1997), producing

[1] Dept. of Geological Sciences, Univ. of Colorado, Boulder, CO, 80309; robin@globalecology.stanford.edu
[2] Dept. of Global Ecology, Carnegie Inst. of Washington, Stanford, CA 94305; greg@globalecology.stanford.edu
[3] Dept. of Geological and Environmental Sciences, Stanford Univ., Stanford. CA 94305

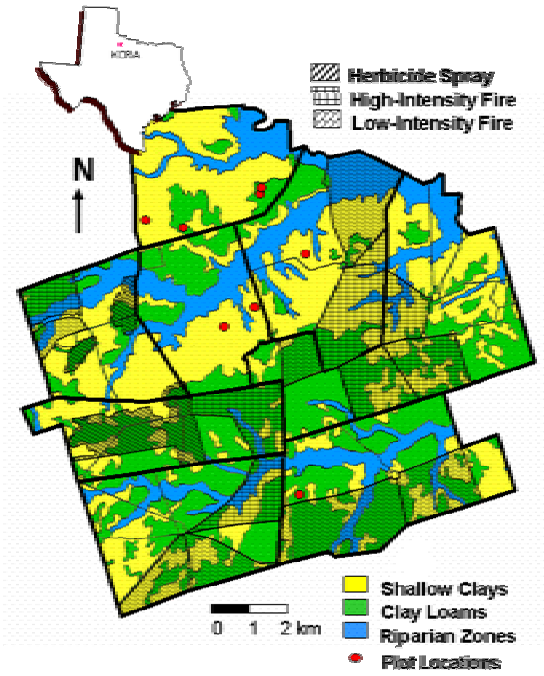

Figure 1. Pasture and soil map for Kite Camp Research Area (KCRA), Vernon, TX showing two dominant soil types and the riparian areas. Red circles mark locations where field measurements of soil NO fluxes were collected. Pastures experiencing prescribed fire and herbicide treatments prior to airborne imaging are hatched; non-hatched areas have no known brush management since at least the 1950s.

landscape mosaics of grassland, savanna (< 800 stems ha^{-1}) and woodland (up to 7,100 stems ha^{-1}) (Hughes et al. 1999).

3. Airborne Imaging Spectrometry.

Airborne imaging spectrometer data were collected on September 29, 2001 over a 140 km^2 region of Waggoner Ranch. The September time period afforded the greatest contrast between the woody *Prosopis* which were full and green and the herbaceous layer, which had senesced (Asner et al. 1998, Asner et al. 2003b). The NASA Airborne Visible and Infrared Imaging Spectrometer (AVIRIS) was flown onboard a Twin Otter aircraft at an altitude of 4000 m, providing image data with a 3.3 m spatial resolution. The data were geo-rectified using an onboard global positioning-inertial navigation system (GPS-INS) and a post-processing algorithm developed by (Boardman 1999). Eleven flightlines were then mosaicked using an algorithm developed by Asner et al. (2003b). AVIRIS data were then atmospherically corrected using the FLAASH algorithm (Matthew et al. 2000).

4. Spectral Mixture Analysis.

The spectral mixture model AutoMCU (Asner and Lobell 2000, Asner and Heidebrecht 2002) was used to calculate estimates of green photosynthetic vegetation (PV), senescent non-photosynthetic vegetation (NPV) and bare soil covers within each pixel, along with statistical uncertainty estimates for each cover type using an automated Monte Carlo uncertainty analysis. AutoMCU uses three endmember "bundles" of PV, NPV and soil, derived from an extensive endmember database for North American drylands (Asner et al. 1998, Asner et al. 2000), to decompose each image pixel using the following equation:

$$\rho_{pixel} = \Sigma[C_e * \rho_e] + \varepsilon = [C_{PV} * \rho_{PV} + C_{NPV} * \rho_{NPV} + C_{soil} * \rho_{soil}] \quad (1)$$

$$\Sigma C_e = 1.0 \quad (2)$$

where ρ is the reflectance factor, C is the cover fraction for each endmember, PV is photosynthetically active vegetation, NPV is non-photosynthetically active vegetation, and ε is the error term. Equation (2) constrains the sum of the fractions to one. On a pixel by pixel basis, the AVIRIS reflectance measurements were spectrally unmixed 50 times using PV, NPV and soil spectra randomly selected from each endmember bundle. The Monte Carlo approach was used to calculate both mean fractional cover values of PV, NPV and soil on a per-pixel basis, and to compute absolute errors in estimates of these cover types, reported as standard deviations. AVIRIS-derived estimates of PV were compared to field-based measurements of aboveground *Prosopis* canopy cover (from Asner et al. 2003a) to determine if this remotely sensed variable could be used to spatially extrapolate NO emissions across the region (Figure 2).

5. Field N Oxide Measurement and Extrapolation Incorporating AVIRIS predicted Woody Vegetation Cover

Soil NO flux measurements are documented in detail in Martin et al., (in press). Briefly, six field campaigns were conducted approximately bi-monthly from May 2000 to June 2001 on nine 60 x 60 m plots spanning a range of landscape units that have been previously characterized for soil texture, plant canopy cover, and standing biomass through remote sensing and ground-based measurements (Asner et al., 1998; Hughes et al., 1999). Fluxes were measured from six PVC chambers at each plot. Measurements were stratified at each site beneath tree canopies (n = 3) and in grass interspaces between canopies (n = 3).

Soil NO flux exhibited a strong linear relationship with *Prosopis* cover (Figure 3; Martin et al., in press). Based on this relationship, we extrapolated NO fluxes on a pixel by pixel basis as they related to the AVIRIS estimated *Prosopis* cover producing a spatially explicit map of NO flux. Error in the prediction of NO flux was calculated for each pixel as:

$$Total\ Spatial\ Error = \sqrt{(PV\ error)^2 + (NO\ error)}$$

where, PV error is the uncertainty in estimation of the PV cover fraction derived from Monte Carlo calculation in the spectral mixture analysis, and NO error is the standard error of NO relationship with *Prosopis* cover as:

$$NO\ error = \sigma^2 \left[1 + \frac{1}{n} + \frac{\left(x^* - \bar{x}\right)^2}{S_{xx}} \right]$$

where σ^2 is the standard error in the regression estimate between field measurements of PV cover fraction and NO emissions, n is the number of samples in the image, x^* is the PV cover fraction of a given pixel, $\bar{x}$ is average PV cover measured in the field plots, and S_{xx} is the sum of squares of the error in the PV cover measured in the field plots.

6. Comparison of Regional Estimates

Estimates of NO emissions derived from the different calculation methods were compared: 1) simple averaging of all field data, 2) averaging of only the summer field measurements assuming NO is not produced during the months with low temperatures, 3) spatially extrapolating NO fluxes using a woody vegetation map derived from imaging spectrometer observations. The covariance was calculated for each estimate so that variation between methods could be assessed independent of sample size differences.

7. Results and Discussion

Soil nitrogen oxides are a broad indicator of the overall N balance of an ecosystem (Davidson et al. 2000). Regional studies of N oxide emissions from savanna soils

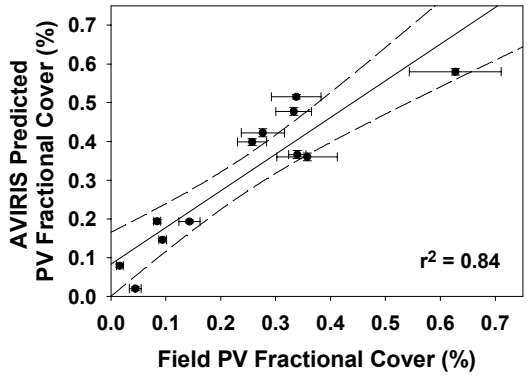

Figure 2. Relationship between woody *Prosopis* cover in georeferenced 60 x 60 m plots estimated from AVIRIS measurements collected in 2000 and field canopy measurements. Solid line shows the regression relationship used to adjust satellite estimates of PV cover (Estimated PV cover = 0.95 * Field PV Cover + 0.08). Dashed line depicts 95% confidence interval in the prediction of the regression. Vertical error bars indicate uncertainty in Monte Carlo analysis and co-location of AVIRIS pixels within field plots. Horizontal error bars indicate variability in belt-transect cover estimates within field plots (Asner et al. 2003a).

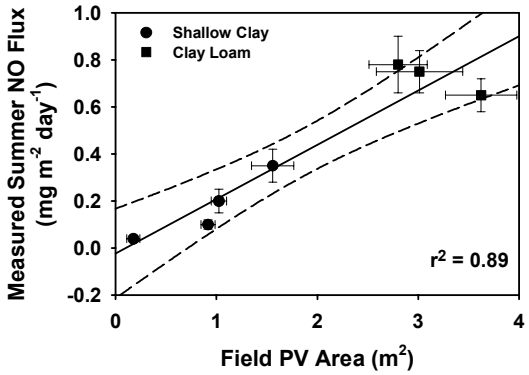

Figure 3. Relationship between NO flux and PV cover measured within field plots indicated in figure 1. Solid line show the regression relationship used to calculate NO emissions on a pixel by pixel basis as they relate to woody canopy cover across the region (NO flux = 0.23 * AG *Prosopis* cover – 0.02). Dashed line depicts 95% confidence interval in the prediction of the regression. Vertical error bars indicate standard error in NO field measurements. Horizontal error bars indicate variability in belt-transect cover estimates within field plots (Asner et al. 2003a).

are challenged by the great spatial and temporal heterogeneity in the processes regulating these emissions. Numerous studies report increases in woody plant cover in savanna ecosystems, most of which focus on classification and quantification of vegetation structure (Buffington and Herbel 1965, Harrington and Harman 1995, Ansley et al. 2001, Moleele et al. 2002, Asner et al. 2003a). Many plot-scale studies suggest that changes in canopy structure are translated to biogeochemical changes in the soil, specifically in the C and N stores (Archer et al. 2001, Asner et al. 2003b). N oxide emissions are subsequently related to N capital, which can be linked to plant cover and growth (Aber and Melillo 1991, Vitousek and Howarth 1991). This study aimed to capitalize on relationships between remotely sensed, spatially-distributed properties of vegetation and soil, and climatic controls (temperature and precipitation), to provide estimated regional variations in NO emissions from rangeland soils.

Spatial Patterns in Woody Cover

Prosopis glandulosa occurs on more than 20 million ha of rangeland in Texas, with documented increases over the past 100 y (Teague et al. 1997, Ansley et al. 2001, Asner et al. 2003a). The distribution and structure of *Prosopis* cover, and related biogeochemical properties, is a function of many of variables. Climate establishes the biogeographical setting, with seasonal temperature variations and limited rainfall promoting the co-evolution of woody communities and grasses. Accurate prediction of woody canopy cover is the key step to understanding the regional distribution of soil NO emissions as they respond to these controlling factors.

Fractional cover estimates of photosynthetic vegetation (PV), non-photosynthetic vegetation (NPV) and bare soil derived from AVIRIS reflectance measurements varied substantially across the study region (Figure 4). AVIRIS-derived fractional cover estimates of woody vegetation were well correlated to field measurements (r^2 = 0.84, p <0.01; Figure 2). Woody *Prosopis* cover (shades of red) was higher on the deeper clay loam soil than on the shallow clay soils, with values of 35 and 25%, respectively ($p < 0.001$, t-test). The areal extent of these two soil types was similar throughout the region, approximately 56 and 59 km^2 for shallow clay and clay loam, respectively, leading to an average regional woody cover of 30%. The standard deviation in predicted PV cover was low (0-9%). Averaged by soil type, the error was approximately 10% of the cover fraction for both soil types, indicating high confidence in the detection of woody plants within the AVIRIS pixels.

Remotely sensed NPV cover was slightly higher on clay loam than on shallow clay soils, with values of 57 and 51%, respectively. Areas of highest NPV cover (shades of green) were found on the upland clay loam soils, in the transition separating areas close to the riparian zones (in black) with high woody cover to the shallow clay areas with little cover (Figure 4). The standard deviation in predicting NPV was 0-10%, similar to that for PV. The bare soil fraction was higher on the shallow clay (42%) than on the clay loam soils (31%) ($p < 0.001$, t-test). The error in predicting the soil fraction was lower than that of PV or NPV (0-2%), indicating the clear detection of this land-surface component.

Using Landsat 7 ETM+ data at 30 x 30 m spatial resolution, Asner et al. (2003a) showed similar areal distributions of woody cover, but averages by soil type differed (48% and 33% on clay loam and shallow clay soils, respectively). They estimated a 23% increase in woody cover across the region over a 63 y period (1937 to 1999), and indicated a trend towards increasing spatial homogeneity of woody cover. The current analysis quantified similar heterogeneous distributions in woody cover in 1999.

The ~10% difference in woody fractional cover between the two studies is most likely do to

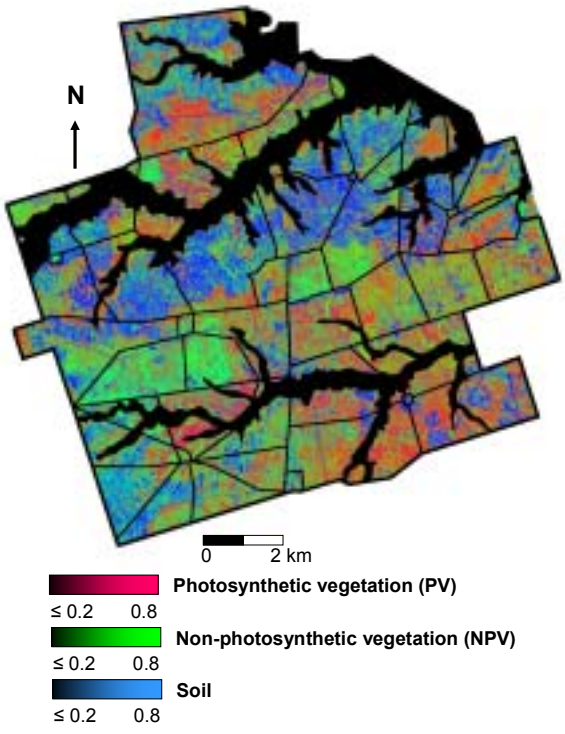

Figure 4. Regional mosaic of spectral unmixing results derived from AVIRIS measurements. Fractional surface cover of PV, NPV, and bare soil are shown in shades of red, green and blue respectively. Riparian areas have been removed. Fences enclosing pastures and the KCRA boundary are shown with black lines.

variation in plant phenology caused by interannual variation in precipitation. The September over-flights were chosen in both studies to maximize senescence of the herbaceous canopy, while the woody canopies remained fully green at the time of imaging. However, differences in the greenness of both woody and herbaceous vegetation occurred due to differences in precipitation during the preceding months in each study. On average, precipitation in the Waggoner Ranch region ranged from 400 to 900 mm over the last 10 y (NOAA, 2001). The 2001 season had extremely low rainfall (410 mm) and followed the summer drought of 2000 (no precipitation from July – September). In contrast, rainfall in 1999 during the Landsat study by Asner et al. (2003a) was average (620 mm). This suggests that our estimates of woody cover in this study are conservative, thus NO flux calculations incorporate woody vegetation cover may represent the lower limit for NO emissions in this region. Despite a difference in means, the slope and minimum value between field validation data and estimated woody cover were similar between the two studies (Figure 2; $p < 0.001$; t-test).

Spatial Variations in Soil NO Emissions

Due to the intensive amount of field work involved in the collection of soil trace gas flux data, a true random sampling over the entire area of a given biome is not feasible. In an attempt to characterize the spatial variability within a biome, measurements are often divided equally across soil type, vegetation cover or landscape position. The linkages between woody fractional cover and biogeochemical processes offers a way to capitalize on the power of remote sensing (in this case airborne imaging spectroscopy) to extend a limited number of plot-scale measurements to a regional area. If the distal controls that are remotely observable can be linked to N trace gas emissions, then greater confidence in the overall emissions estimates from the region can be achieved.

Our recent field study identified woody vegetation as the key spatial control over NO emissions following woody encroachment in North Texas (Martin et al. in press). A variety of NO emission rates associated with canopy cover types (woody versus herbaceous) have been documented in other studies. These range from small differences (~ 10%) in emissions measured under or away from mesquite canopies in southern New Mexico (Hartley and Schlesinger 2000) to a doubling in NO emissions following an increase in aboveground biomass and a doubling of total soil N from two savanna sites in South Africa (Levine et al. 1996, Parsons et al. 1996). Similarly, higher litter quality from an N-fixing legume contributed to increased N cycling and higher NO emissions in a Puerto Rican forest (Erickson et al. 2002).

Extrapolation of soil NO emissions using the photosynthetic vegetation (PV) cover, measured by AVIRIS and modeled by AutoMCU, highlighted a high degree of spatial variability across the study region with emissions ranging from 0 to 2.5 mg m^{-2} d^{-1} (Figure 5a). The extremes in predicted NO flux were then obvious, with lowest

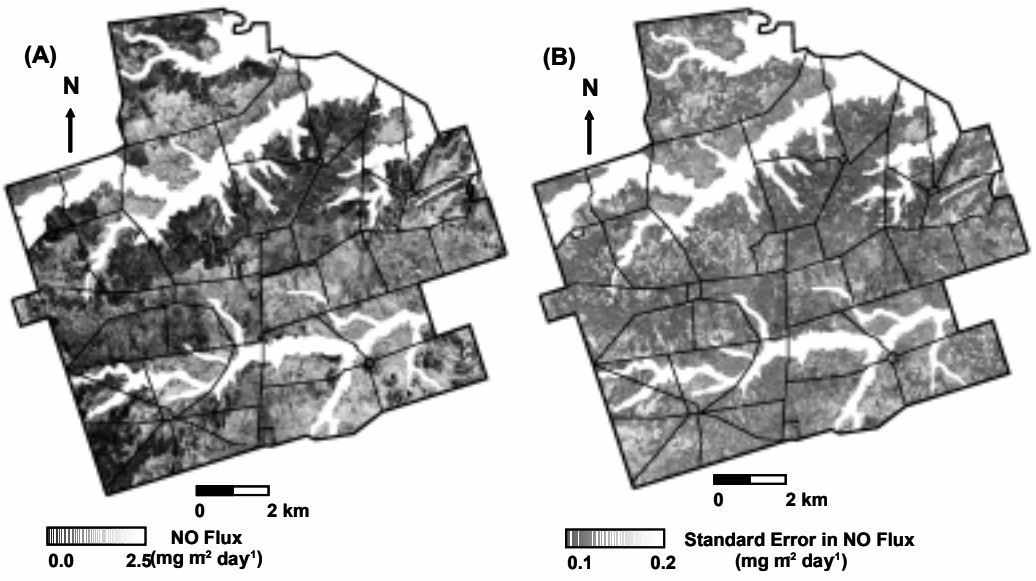

Figure 5. Regional map of NO emissions (A) and associated error (B). Brighter areas represent higher NO flux values. Riparian areas, indicated in white, were not included in the analysis. Fences enclosing pastures and the KCRA boundary are shown with black lines.

NO values in areas of high bare soil fractions (shades of blue, Figure 4) and highest values closer to the riparian zones containing dense canopies (black regions). The total error of NO flux estimates varied between 0.2 – 0.6 mg m^{-2} d^{-1}. Spatially, the error in estimation was higher at the extremes of woody cover values (Figure 5b).

Remote sensing highlighted the stratification of NO emissions by soil type, with higher emissions from clay loam than from shallow clays soils (5a). NO emissions measured in the field and averaged by soil type followed the same pattern (Table 1). Soil texture affects the production and emission of NO by influencing both N availability (plant growth and subsequent litter turnover) and soil porosity (emission path length and water-holding capacity; (Firestone and Davidson 1989, Robertson et al. 1989). In this system, NO emissions co-vary with vegetation change across soil type.

Evaluating regional NO emissions by soil type illustrates the benefit of incorporating remote sensing data in biogeochemical studies. On an area-integrated basis, the estimate for this region (120 km^2), based on stratification by soil type alone, estimated NO emissions by approximately 4 Mg NO-N y^{-1}. This value was nearly a third of the total annual flux calculated after accounting for the spatial variability of woody vegetation cover (14 Mg NO-N y^{-1}). The largest difference appeared in the estimation of emissions from shallow clay soils, producing a 260% difference when spatial variability was included (Table 1). In contrast, there was little change in the estimation of NO flux from clay loam soils. This difference in calculated NO emissions by soil type arises because the PV cover measured in the field plots located on shallow clay soil was lower (8%) than that of the entire region (25%). This difference would remain undetected without the aid of imaging spectroscopy data, which extended the estimation of vegetation fractional cover to the entire region.

8. Conclusions

Our study demonstrates the advantage of using remote sensing to characterize the spatial heterogeneity in ecosystem parameters at a scale (meters) commensurate with field-based measurements of these properties. Woody vegetation encroachment provided an opportunity to capitalize on detection of the remotely-sensible parameter of woody cover as it relates to belowground biogeochemical processes that determine N trace gas production. The first spatially-explicit estimates of NO flux were calculated based on *Prosopis* fractional cover derived from high resolution remote sensing estimates of fractional woody cover (< 4m) for a 120 km^2 region of North Texas.

Table 1. Estimated mean annual NO Flux for the entire region (120 km^2) and divided by soil type. Means and coefficient of variation are given.

	Total Area		Shallow Clay		Clay Loam	
Calculation Method	NO flux (mg m^{-2} y^{-1})	CV	NO flux (mg m^{-2} y^{-1})	CV	NO flux (mg m^{-2} y^{-1})	CV
1) all chamber measurements	89.8	1.4	42.6	1.6	137.1	1.3
2) summer chamber measurements (220 days)	86.1	1.0	38.8	1.2	133.9	0.9
3) AVIRIS vegetation map (220 days)	122.0	0.7	100.5	0.8	144.8	0.6

Differences in regional annual NO estimates calculated from traditional extrapolation methods with and without climate variability were compared to estimates calculated using spatially-explicit information on woody vegetation cover derived from remotely sensed data. Incorporating spatial variability nearly doubled the mean annual NO emissions over those estimated from field measurements alone, yielding an annual emission rate of 122 kg NO-N km^{-2} y^{-1} from the region. This emission rate is about half the total wet deposition rate (300-400 kg N km^{-2} y^{-1}; (NADP/NTN) and only a tenth of the estimated N fixed by *Prospis* in the region (600-3000 kg N km^{-2} y^{-1}; (Cleveland et al. 1999).

The spatially distributed nature of the data revealed discrepancies in total estimated NO emissions by soil type, due primarily to limited sampling on shallow clay soils. Spatially-explicit data also permitted the evaluation of the long-term effects of brush management on estimated NO emissions, an otherwise extremely labor intensive process. These data revealed that brush management may significantly decrease NO emissions once short-term variations due to the initial disturbance have dissipated.

9. Acknowledgements.

We thank J. Ansley, S. Archer, K. Heidebrecht, A. Mosier and A. Warner for their technical and logistical assistance. This study was supported by the NASA Earth System Science Fellowship Program (ESS/00-0000-

0188), NASA New Investigator Program (NIP) grant NAG5-8709, and NASA New Millenium Program (NMP) grant NCC5-480 and NCC5_481.

10. References.

Aber, J. D., and J. M. Melillo. 1991. Terrestrial Ecosystems. Saunders College Publishing, Philadephia.

Ansley, R. J., X. B. Wu, and B. A. Kramp. 2001. Observation: Long-term increases in mesquite canopy covering North Texas. Journal of Range Management **54**:171-176.

Archer, S. 1994. Woody plant encroachment into southwestern grasslands and savannas: rates, patterns, and proximate causes. Pages 13-68 *in* M. Vavra, W. A. Laycock, and R. D. Pieper, editors. Ecological Implications of Livestock Herbivory in the West. Society for Range Management, Denver.

Archer, S., T. W. Boutton, and K. A. Hibbard. 2001. Trees in grasslands: Biogeochemical consequences of woody plant expansion. *in* E.-D. Shultze, S. P. Harrison, M. Meimann, E. A. Holland, J. Lloyd, I. C. Prentice, and D. S. Schimel, editors. Global Biogeochemical Cycles in the Climate System. Academic Press, San Diego.

Asner, G. P., S. Archer, R. F. Hughes, R. J. Ansley, and C. A. Wessman. 2003a. Net changes in regional woody vegetation cover and carbon storage in Texas rangelands, 1937-1999. Global Change Biology **9**:1-20.

Asner, G. P., C. E. Borghi, and R. A. Ojeda. 2003b. Desertification in Central Argentina: Changes in ecosystem carbon and nitrogen from imaging spectrometry. Ecological Applications.

Asner, G. P., and R. O. Green. 2001. Imaging spectroscopy measures desertification in the Southwest U.S. and Argentina. EOS Transactions **82**:601-606.

Asner, G. P., and K. B. Heidebrecht. 2002. Spectral unmixing of vegetation, soil and dry carbon in arid regions: Comparing multi-spectral and hyperspectral observations. International Journal of Remote Sensing **23**:400-410.

Asner, G. P., and D. B. Lobell. 2000. A biogeophysical approach for automated SWIR unmixing of soils and vegetation. Remote Sensing of Environment **74**:99-112.

Asner, G. P., C. A. Wessman, C. A. Bateson, and J. L. Privette. 2000. Impact of tissue, canopy and landscape factors on reflectance variability in spectral mixture analysis. IEEE Transactions on Geoscience and Remote Sensing **38**:1083-1094.

Asner, G. P., C. A. Wessman, and D. S. Schimel. 1998. Heterogeneity of savanna canopy structure and function from imaging spectrometry and inverse modeling. Ecological Applications **8**:1022-1036.

Boardman, J. W. 1999. Precision geocoding of low altitude AVIRIS data: Lessons learned in 1998. *in* Eigth JPL Airborne Earth Science Workshop.

Boutton, T. W., S.R. Archer, A. J. Midwood. 1999. Stable isotopes in ecosystem science: Structure, function and dynamics of subtropical savanna. Rapid Communications in Mass Spectrometry **13**:1263-1277.

Buffington, L. C., and C. H. Herbel. 1965. Vegetational changes on a semiarid grassland range. Ecological Monographs **35**:139-164.

Cleveland, C. C., A. R. Townsend, D. S. Schimel, H. Fisher, R. W. Howarth, L. O. Hedin, S. S. Perakis, E. F. Latty, J. C. Von Fischer, A. Elseroad, and M. F. Wasson. 1999. Global patterns of terrestrial biological nitrogen (N_2) fixation in natural ecosystems. Global Biogeochemical Cycles **13**:623-645.

Davidson, E. A., M. K. Keller, H. E. Erickson, L. V. Verchot, and E. Veldkamp. 2000. Testing a conceptual model of soil emissions of nitrous and nitric oxides. Bioscience **50**:667-680.

Erickson, H. E., E. A. Davidson, and M. K. Keller. 2002. Former land-use and tree species affect nitrogen oxide emissions from a tropical dry forest. Oecologia **130**:297-308.

Firestone, M. K., and E. A. Davidson. 1989. Microbiological basis of NO and N2O production and consumption in soil. Pages 7-21 *in* M. O. Andrea and D. S. Schimel, editors. Exchange of Trace Gases Between Terrestrial Ecosystems and the Atmosphere. Wiley and Sons, New York.

Fisher, C. E., C. H. Meadors, R. Behrens, E. D. Robinson, P. T. Marion, and H. L. Morton. 1959. Control of mesquite on grazing lands. Texas Agricultural Experiment Station Bulletin **935**.

Green, R. O., M. L. Eastwood, C. M. Sarture, T. G. Chrien, M. Aronsson, B. J. Chippendale, J. A. Faust, B. E. Pavri, C. J. Chovit, M. S. Solis, M. R. Olah, and O. Williams. 1998. Imaging spectroscopy and the Airborne Visible Infrared Imaging Spectrometer (AVIRIS). Remote Sensing of Environment **65**:227-248.

Harrington, J. A., Jr., and J. R. Harman. 1995. Climate and vegetation in Central North America: Natural patterns and human alterations. Ecology Economy and Environment **5**:135-148.

Hartley, A. E., and W. H. Schlesinger. 2000. Environmental controls on nitric oxide emissions from northern Chihuahuan desert soils. Biogeochemistry **50**:279-300.

Hibbard, K. A., S. Archer, D. S. Schimel, and D. V. Valentine. 2001. Herbaceous biomass dynamics and net primary production accompanying woody plant encroachment in a subtropical savanna. Ecology **82**:1999-2001.

Hoffman, W. A., and R. B. Jackson. 2000. Vegetation-climate feedbacks in the conversion of tropical savanna to grassland. Journal of Climate **13**:1593-1602.

Hughes, R. F., J. B. Kauffman, and V. J. Jaramillo. 1999. Biomass, carbon, and nutrient dynamics of secondary forests in a humid tropical region of Mexico. Ecology **80**:1892-1907.

Levine, J. S., E. L. Winstead, D. A. B. Parsons, M. C. Scholes, R. J. Scholes, W. R. Cofer III, D. R. Cahoon Jr., and D. I. Sebacher. 1996. Biogenic soil emissions of nitric oxide (NO) and nitrous oxide (N_2O) from savannahs in South Africa: The impact of wetting and burning. Journal of Geophysical Research **101**:23689-23697.

Martin, R. E., G. P. Asner, A. R. Mosier, and R. J. Ansley. in press. Effects of Woody Encroachment on Soil Nitrogen Oxide Emissions in a Temperate Savanna. Ecological Applications.

Matson, P. 1997. NOx emission from soils and its consequences for the atmosphere: critical gaps and research directions for the future. Nutrient Cycling in Agroecosystems **48**:1-6.

Matthew, M. W., S. M. Adler-Golden, A. Berk, S. C. Richtsmeier, R. Y. Levin, L. S. Bernstein, P. K. Acharya, G. P. Anderson, G. W. Felde, M. P. Hoke, A. Ratkowski, H.-H. Burke, R. D. Kaiser, and D. P. Miller. 2000. Status of atmospheric correction using a MODTRAN4-based algorithm. Pages 199-207. *in* SPIE Proc. Algorithms for Multispectral, Hyperspectral, and Ultraspectral Imagery, VI.

Moleele, N. M., S. Ringrose, W. Matheson, and C. Vanderpost. 2002. More woody plants? the status of bush encroachment in Botswana's grazing areas. Journal of Environmental Management **64**:3-11.

NADP/NTN. National Atmospheric Deposition Program (NRSP-3)/ National Trends Network,. Natural Resource Ecology Laboratory, Colorado State University, Fort Collins, Colorado.

NOAA. 2001. Climatological data, 1970-2000, National Oceanic and Atmospheric Administration National Climatic Data Center.

Parsons, D. A. B., M. C. Scholes, R. J. Scholes, and J. S. Levine. 1996. Biogenic NO emissions from savanna soils as a function of fire regime, soil type, soil nitrogen, and water status. Journal of Geophysical Research **101**:23,683-623,688.

Robertson, G. P., M. O. Andreae, H. G. Bingemer, P. J. Crutzen, R. A. Delmas, J. H. Duyzer, I. Fung, R. C. Harriss, M. Kanakidou, M. K. Keller, J. M. Melillo, and G. A. Zavarzin. 1989. Group report, Trace gas exchange and the chemical and physical climate: Critical interactions. Pages 303-320 *in* M. O. Andreae and D. S. Schimel, editors. Exchange of Trace Gases Between Terrestrial Ecosystems and the Atmosphere. John Wiley and Sons, Chichester, England.

Rundel, P. W., E. T. Nelson, M. R. Sharifi, R. A. Virginia, W. M. Jarrell, D. H. Kohl, and G. B. Shearer. 1982. Seasonal dynamics of nitrogen cycling for a *Prosopis* woodland in the Sonoran Desert. Plant and Soil **67**:343-353.

Scholes, R. J., and S. R. Archer. 1997. Tree-grass interactions in savannas. Annual Review of Ecology and Systematics **28**:517-544.

SCS. 1962. Soil Survey of Wilbarger County, Texas. 18, United States Department of Agriculture\Soil Conservation Service, Fort Worth, TX.

Teague, R., R. Borchardt, J. Ansley, B. Pinchak, J. Cox, J. K. Fox, and J. McGrann. 1997. Sustainable management strategies for mesquite rangeland: the Waggnor Kite Project. Rangelands **19**:4-8.

Vitousek, P. M., and R. W. Howarth. 1991. Nitrogen limitation on land and in the sea: How can it occur? Biogeochemistry **13**:87-115.